Influence of Silica Reinforcement upon the Glass Transition Behavior of Acrylic Polymers

CHARLES G. REID* and ALAN R. GREENBERG, *Department of Mechanical Engineering, University of Colorado, Box 427, Boulder, Colorado 80309-0427*

Synopsis

The glass transition temperatures (T_g) of poly(acrylic acid), poly(methyl acrylate), and poly(ethyl acrylate) filled with submicron particulate silicas and silicates have been measured by dynamic mechanical spectroscopy and differential scanning calorimetry. The peak temperatures of the damping factor ($\tan\delta$) and the dynamic shear loss modulus (G'') were shifted by an amount which depended upon the quantity and type of filler added to each polymer. The temperatures corresponding to the step discontinuity of specific heat also shifted, but to a lesser extent than those measured mechanically. The degree of T_g shift per unit of volumetric filler addition increased with polymer pendant group polarity for both measurement methods. Utilizing a T_g-crosslinking analogue, a model was developed that related positive T_g shifts to polymeric segmental adsorption onto filler surfaces. This model also incorporated negative contributions to the T_g shift from energy storage mechanisms arising from particle–particle interactions, as well as corrections due to effective surface area available for polymer adsorption.

INTRODUCTION

The rubber industry has long utilized the addition of finely divided particulate fillers, such as carbon blacks and silicas, to polymeric materials as a means of enhancing elastomeric mechanical behavior. Such reinforcement is differentiated from pigmentation or volume loading in that the latter produces no significant improvement of the material's mechanical properties. Studies of reinforcement indicate that stress is effectively transferred between the matrix and embedded particulate phases over an interfacial region of finite dimensions.[1] The morphological changes of the matrix material that have been associated with the formation of such an interfacial region include chain conformation alteration, adsorptional network formation (with the particles as nodes), and particulate surface-induced crystallization.[1,2]

Several authors have hypothesized that the addition of particulate fillers to a polymeric matrix can reduce chain mobility in the vicinity of the particle surface.[2-5] Mechanically and thermally determined transition temperatures (e.g., glass or melting transitions) provide insight into polymeric molecular mobility and are sensitive to physical hindrances arising from crosslinking, bulky pendant groups, and various intermolecular interactions. Studies of these effects upon the glass transition temperature (T_g) are well documented in literature reviews.[6,7] If the interfacial regions of filled polymers are immobilized by interaction with filler surfaces, then the T_g of these molecules should be increased. NMR measurements on filled polymers by other investigators

*Current address: Union Carbide Corporation, Weston Canal Center, P.O. Box 450, Somerset, NJ 08875-0450.

Journal of Applied Polymer Science, Vol. 39, 995–1014 (1990)
 CCC 0021-8995/90/040995-20$04.00

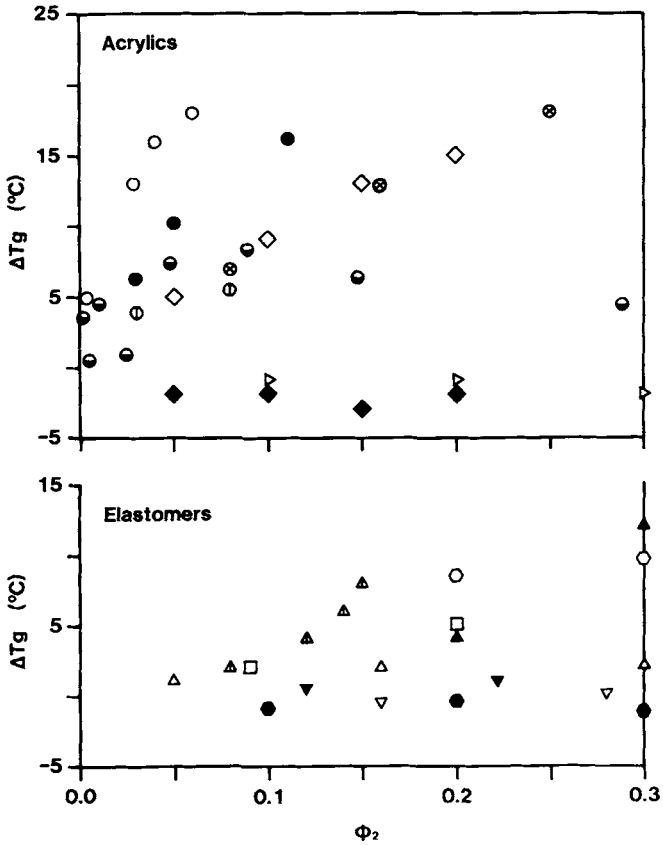

Fig. 1. Reported values of T_g shift plotted by composite filler volume fraction (ϕ_2) for acrylic (top) and elastomeric (bottom) polymers: poly(methyl methacrylate) (PMMA) and fumed silica (FS) composites measured by calorimetry (○)[2], dynamic mechanical spectroscopy (DMS) (●)[14], dielectric relaxation (⊙)[14], and differential scanning calorimetry (DSC) midpoint (◒)[11]; PMMA–mica flake composite measured via 10 Hz DMS (⊗)[12]; poly(hydroxyethyl methacrylate)–glass beads (GB) via torsion pendulum (▷)[18]; PAA–FS (◆) and PAA–calcium silicate (◇) via 3 Hz DMS[16]; poly(dimethylsiloxane)-FS via calorimetry (△)[2], torsion pendulum tan δ (▲)[5] and dilatometry (⧋)[15]; polyisobutylene–GB (□) and polyurethane–GB (○) via linear expansion coefficient[13]; styrene–butadiene rubber filled with carbon blacks HAF (▽) and MT (▼) via dilatometry[17]; polyurethane–sodium chloride via dilatometry (⬣).[19]

have confirmed that there is reduced segmental mobility at or near the filler particles.[2,8,9] Consequently, as the interfacial region is intimately mixed with the matrix material, the bulk T_g may be shifted in a manner similar to that observed for compatible polymer blends.[6,10]

Many instances of increased bulk T_g of particulate-filled polymers have been reported.[2-5,11-17] Representative data for a variety of filled acrylic polymers and elastomers are shown in Figure 1. The change in T_g relative to the T_g of the unfilled matrix (T_{g_0}) is defined as

$$\Delta T_g = T_g(\phi_2) - T_{g_0} \tag{1}$$

and is plotted in Figure 1 versus the volume fraction of filler ϕ_2. These data indicate that the values of ΔT_g vary considerably, even for identical

polymer–filler combinations.[2,11,14] In addition to increases of T_g, certain systems exhibit decreases or no change of T_g with increasing filler content.[16–19] From Figure 1, a systematic dependence of the increase of T_g upon ϕ_2 cannot be easily discerned. In fact, the choice of ϕ_2 as the independent variable is somewhat arbitrary, although many data sets have traditionally been presented in this manner.

In an extensive literature review, Manson and Sperling[10] concluded that for filled polymers that exhibited changes in T_g, the magnitude of the shift depended upon the nature of the filler surface and the resulting interaction between the particulate and polymer phases. Toussaint[20] has classified T_g changes according to three different types of interactions: hydrodynamic, physical adsorption, and chemisorption. These interactions shift T_g by an amount that depends upon the volume fraction of filler for hydrodynamic effects, and the amount of available filler surface area for adsorptional effects. Surface area aspects are most often studied as a function of particle size variation, and several investigators have measured larger increases of T_g with smaller particles at constant volumetric content.[12,17,21]

Based upon the above studies, the T_g of a particulate-filled polymer is partly determined by the amount of surface area available for polymer–filler interaction. Several models that describe T_g shifts of filled polymers have been reported, some of which consider surface area contributions. The empirical relations of Droste and DiBenedetto[3] and Fritschy and Papirer,[4] compared previously,[16] relate T_g to exponential functions of ϕ_2 and empirical constants computed for specific polymer–filler systems. However, only the relation of Fritschy and Papirer explicitly considers surface area parameters based upon nominal properties of the filler.

Lipatov and co-workers[2,14] have proposed a physical model whereby a boundary layer surrounds an embedded filler particle. This layer exhibits distinctively different thermal, chemical, and mechanical properties with respect to the matrix material. Changes in T_g are then related to observed changes in the magnitude of the specific heat step at T_g,[14] assuming that polymeric molecules that interact with the filler are constrained and do not participate in the glass transition process. Thus, depending upon the degree of polymer–filler interaction, the bulk T_g may be increased and specific heat step decreased in a manner similar to the effect of increased crystallinity upon T_g that is observed for certain systems.[2]

Despite their applicability to selected polymer–filler systems, certain limitations are present in the above-mentioned models. These three relationships[3,4,14] describe neither reported decreases of T_g[16–19] nor increases followed by decreases of T_g with increasing filler content[11] (Fig. 1). In addition, evaluation of boundary layer properties must be inferred from the composite bulk properties, as the former may not be obtained independently. However, the determination of inferred properties may be obscured by other factors that alter the bulk matrix material in a manner independent of filler content. Examples of these include measurement methodology, specimen thermal history, processing techniques, and environmental effects. Although there have been many studies of the effects of filler content upon T_g and mechanical properties, few systematic investigations have been conducted in which T_g shifts could be attributed to definable parameters.

The objective of the present study is to consider the nature of T_g shifts for filled polymers as a function of assumed physical and chemical changes on each side of the interfacial region. The acrylic polymer series, poly(acrylic acid) (PAA), poly(methyl acrylate) (PMA), and poly(ethyl acrylate) (PEA), were utilized such that polymer chemistry was effectively altered by changing the polarity and length of the pendant group. The composition (and consequently the inferred surface chemistry) of the fillers utilized was also varied, while maintaining approximately constant surface area and geometric properties. If the predominant interaction mechanism of polymer and filler is via the polymer pendant group, then systematic changes of T_g with the polymer type should occur. To eliminate spurious contributions to the shift of T_g, the processing technique, relative thermal history, and polymer molecular weight were maintained constant for each composition studied.

MATERIALS AND METHODS

Poly(acrylic acid) was obtained in powdered form (Polysciences Inc.) and used as received. PEA and PMA were synthesized from monomer (Aldrich Chemical Co.) by free radical bulk polymerization with 2,2′-azobis(2-methylpropionitrile), as an initiator, in a molar ratio of $[I]/[M] = 3 \times 10^{-4}$. Due to the tendency of lower ester acrylates to chain transfer extensively, 2-butanol was added in a molar ratio of $[S]/[M] = 0.05$ and 0.08 for EA and MA, respectively, to prevent gelation and limit molecular weight.[22] The polymerization reactions were conducted in 10 mm glass tubes suspended in a 60°C circulated oil bath for a minimum of 24 h. All three polymers were subsequently stored under vacuum (i.e., < 700 Pa) at 40°C for several weeks before further use. Polymer solutions were then generated for sample processing; PEA and PMA were mixed with toluene and PAA with ethanol, each at 1:20 by volume.

The particulate fillers utilized were fumed silica (Aerosil OX50), precipitated silica (Durosil), and precipitated calcium-silicate (Extrusil), the properties of which are listed in Table I. Aerosil is primarily used for liquid thickening, elastomer reinforcement, and anticaking agents. Durosil and Extrusil are manufactured especially for rubber and plastics reinforcement. These fillers were chosen due to similarities in their nominal particle size and BET surface area along with apparent differences in surface chemistry. Oil or DBP absorption numbers indicate that there is approximately the same degree of agglomeration for these three fillers. However, the types of agglomerates differ greatly between fumed and precipitated products: Aerosil agglomerates into chains of single particles while Durosil and Extrusil form randomly shaped aggregates several μm in diameter. Thus, the BET surface area for precipitated products is less than expected given the primary particle size due to the exclusion of surface area in the formation of these aggregates. Because the nominal geometric properties were approximately equal for each filler, the filler surface area available for polymer interaction within the composite could theoretically be varied identically via the amount of filler added.

The surface chemistry of pure silicas has been established to consist of silanol (Si—OH) and siloxane (Si—O—Si) groups to which water is reversibly

TABLE I
Filler Characteristics[a]

Property	OX50 (Aerosil)	Durosil	Extrusil
BET Surface Area $\bar{s}$ (m^2/g)	50 ± 15	60	35
Average particle size (nm)	40	25	25
Oil adsorption ($cm^3/100$ g)	150[b]	165[c]	100[d]
DBP absorption[e] (mL/100 g)	250[f]	220	
Density (g/mL) (±0.05)	2.2	1.95[g]	2.10[g]
pH (5% aqueous suspension)	3.8–4.5	9	10
Moisture (wt %)			
2 h at 105°C	< 1.5	6	6
15 min at 500°C[h]	0.2	3	9
Composition (wt %)			
SiO_2	> 99.8	98	91
Al_2O_3	< 0.08	0.2	0.2
TiO_2	< 0.03	—	—
Fe_2O_3	< 0.01	0.03	0.03
HCl	< 0.01	—	—
Na_2O	—	1.0	2
SO_3	—	0.8	—
Cl^-	—	—	0.8
CaO	—	—	6

[a] Product names are registered trademarks of Degussa Corp., data obtained from Refs. 23–25, except as noted.
[b] Estimated value.[26,27]
[c] Data for similar product Hi-Sil EP, PPG Industries, Ref. 27.
[d] Data for similar product Silene EF, PPG Industries, Ref. 28.
[e] Dibutylphthalate adsorption, ASTM D2414.
[f] Estimated value.[25]
[g] Ref. 27.
[h] Via thermogravimetric analysis as described in text.

bound.[26,29] The silanol group is slightly acidic (the hydrogen dissociates easily in water) and has an ideal pH of 4.6. The reported pH for OX50 is lower than this due to the presence of residual contaminants from synthesis (HCl) and adsorption of water.[25,29] For precipitated silica and silicates, the concentration of silanol groups tends to be greater than fumed silica because more of the silanol groups have condensed irreversibly to siloxanes during the high temperature flame processing of fumed silica.[29] However, pH values of precipitated silica tend to be basic due to the presence of unwashed salts that remain from the original sodium silicate solution.[29] We have confirmed the presence of sodium and calcium atoms on or near the surface of Durosil and Extrusil by means of energy dispersive X-ray energy analysis. Thus, surface interaction with polymers can occur via the silanol groups and adsorbed water for both fumed and precipitated silicas, and possibly via ionic species for precipitated silicas.

Composite specimens were prepared by mixing predetermined amounts of vacuum treated fillers with polymer solutions in approximately 20 mL aliquots. The vacuum treatment at 45°C for several days removed all physically adsorbed water.[29] However, transfer of the fillers from the vacuum oven to the

polymer solutions in air undoubtedly allowed some adsorption of water to occur. These suspensions were stirred slowly for several hours and then subjected to ultrasonic agitation with a 10 mm diameter, 20 kHz horn operated at 45 W for 7 min. The processing power and time were optimized for these systems to maximize filler dispersion while minimizing polymer degradation. After casting the suspensions as thin films, solvent was removed by evaporation and the composites were stored under heated vacuum: PEA and PMA specimens at 40°C for several weeks and PAA samples at 110°C for several months. Thermogravimetric analysis (Perkin-Elmer TGS-2) of composite samples removed from the vacuum oven indicated the absence of any residual solvent weight loss prior to the onset of polymer degradation.

Desired sample shapes were obtained by compression molding of the dried films into 2 mm thick rectangular slabs. PEA and PMA composites were molded at 60 and 80°C, respectively, under 25 MPa for 20 min; PAA composites were molded at 165°C under 70 mPa for 10 min. All of the molded specimens were allowed to slowly cool to room temperature in the mold at less than 1 MPa. After removal from the mold, 7 mm disks were cut from the slabs for dynamic mechanical testing. Additionally, unfilled polymer specimens were subjected to the same preparation techniques. The PMA and PEA composites were then stored at 40°C under vacuum, above their individual T_g's, while the PAA composites were stored at 90°C, below their T_g, due to the tendency of PAA to chemically react at elevated temperatures.[30]

Molecular weight characterization of unfilled PEA and PMA was performed with gel-permeation chromatography (GPC) after processing. Measurements were made on 25 μg samples in tetrahydrofuran after calibration with polystyrene standards. Densities of the homopolymers and composites were measured with 10-mL pycnometers at 25°C utilizing hexadecane as the confining fluid. Filler content was determined by sample combustion with a thermogravimetric balance. Samples of approximately 10 mg were heated rapidly from room temperature to 500°C under oxygen purge and held isothermally while the weight loss was monitored until stability was achieved. Control measurements of pure polymer and filler were conducted under identical conditions to determine the residue and weight loss fractions, respectively.

Molecular weights and densities of the three homopolymers are detailed in Table II. Although PAA was not characterized by GPC, the viscosity average molecular weight determined by the vendor is reported. The filler volume fractions and bulk densities of each composite were computed from the filler densities listed in Table I, measured values of filler mass fraction and homopolymer densities. Gross defects or voids within the composites were minimal, as measured composite densities were very close to those calculated from measured filler mass content.

Viscoelastic properties were measured with a Polymer Laboratories Dynamic Mechanical Thermal Analyzer (DMTA), Model Mark-I, in a shear sandwich configuration. Samples were fastened to aluminum platens with a commercial cyanoacrylate cement, and the central platen deflected sinusoidally with an amplitude of 0.015 mm (corresponding to a strain of 0.75%) at discrete frequencies of 0.33, 1, 3, 10, 30, and 90 Hz. PEA and PMA samples were cooled at a rate of 10°C/min with liquid nitrogen to approximately 40°C

TABLE II
Polymer Characteristics

Polymer	$\bar{M}_w$[a] $\times 10^{-5}$	$\bar{M}_n$[a] $\times 10^{-5}$	$\bar{X}_n$	Density (g/cm^3) at 25°C ± 0.01	DMTA 1 Hz log(G') Record at T (Pa)	(°C)
PAA	≈ 4.5[b]		≈ 5000	1.42	5.87	161
PMA	2.4	1.1	1300	1.21	5.75	55
PEA	5.6	2.5	2500	1.11	5.41	20

[a] GPC measurements as described in text.
[b] Viscosity average MW reported by vendor.

below T_{g_0} and subsequently heated at 2°C/min during data collection. PAA samples were heated from room temperature at the same rate. The sample chamber was purged with nitrogen gas at a flow rate of 100 mL/min. Two frequencies were multiplexed for each run under the control of a Hewlett Packard Model 9816 computer. The sample chamber temperature was measured with a platinum RTD, which was calibrated by substituting precision resistors. A modulus calibration was performed by a vendor-recommended technique of mass differences. At least three scans were made at each frequency on different samples; the mean value of the data is reported for each composition.

Differential scanning calorimetry (DSC) (Perkin-Elmer Model DSC-4) was also used to locate the T_g of PEA and PMA composites. Sample size was 10 ± 0.2 mg of polymer, taking into account the mass fraction of filler. All samples were encapsulated in aluminum pans and stored at 40°C under vacuum for 2 days prior to testing. PEA DSC scans were conducted using the following protocol: isothermal at 30°C for 5 min, cool at 10°C/min to −70°C, isothermal for 5 min, and heat at 10°C/min during data collection. PMA was subjected to an identical thermal history, elevated by 30°C. The melting point of mercury (−38.8°C) was used as the temperature calibration point before and after every three scans. Calibration with the melting point of indium (156.6°C), under identical conditions, confirmed that deviation in the range of interest was nearly constant and justified the use of a single point calibration. Samples were used only once and the reported results were based upon the mean of at least three samples of identical composition.

Two standard methods of T_g characterization were utilized for DSC: (1) onset T_g, the extrapolated intersection of the linear heat signal below T_g with the steepest part of the step change near T_g, and (2) midpoint T_g, the intersection of the DSC trace with the bisector of the extrapolated linear signals above and below the transition. The midpoint method has been demonstrated by Flynn[31] to measure transition points that are closer to the thermodynamic definition of T_g, the point of slope discontinuity of the enthalpy–temperature curve.

RESULTS

The T_g of materials measured via dynamic mechanical methods may be determined via several means. The two most commonly used methods are

TABLE III
Unfilled Homopolymer Transition Temperatures

Technique	T_{g_0} (°C)		
	[PAA][a]	[PMA]	[PEA]
DMTA 1 Hz			
tan δ peak	131 ± 2(135)[b]	25 ± 2(26)[c]	−10 ± 2(−5)[d]
G'' peak	117 ± 3(125)[e]	17 ± 2(22)[c]	−20 ± 3(−25)[f]
DSC			
Onset	(114)[g]	14.2 ± 0.7(10)[h]	−20.0 ± 0.7(−24)[h]
Midpoint		16.0 ± 0.7	−18.1 ± 0.8

[a] Previously published values in parentheses.
[b] 3 Hz DMTA in bending.[16]
[c] Torsion pendulum.[32]
[d] Sonic attenuation peak.[33]
[e] 3 Hz DMTA in bending.[34]
[f] Torsion pendulum.[35]
[g] DSC 10°C/min onset.[36]
[h] Dilatometry.[37]

primary relaxation peak temperatures of the tangent of the loss angle (tan δ) or the dynamic shear loss modulus ($G'' = G' \cdot \tan\delta$), at constant frequency. The 1 Hz tan δ and G'' peak temperatures for PAA, PMA, and PEA homopolymers are summarized in Table III. The errors given for these values include the standard deviation of the mean, calculated from multiple measurements, plus an additional systematic error of ±2°C attributed to thermal gradients within the sample chamber and thermal lag of the sample. Previously published values of mechanically measured T_g for PAA, PMA, and PEA homopolymers agree favorably with those reported in Table III. For the comparison of T_g between filled and unfilled specimens, the systematic error was assumed to be constant and primarily a function of the measurement technique, such that the relative change of T_g (ΔT_g) contained only random error.

Representative DMTA measurements are shown in Figure 2 for the PEA–Extrusil system. Measured values of dynamic shear storage modulus (G') below the transition region are lower than the actual modulus by a factor of approximately 0.1 due to inherent limitations of the DMTA to measure stiff materials in shear. Above the transition, however, G' values were accurate to within the capabilities of the instrument. For materials that demonstrated a positive shift of tan δ peak temperatures, such as the PEA–Extrusil system shown, the G' transition region not only shifted vertically (reinforcement effect), but also horizontally to higher temperatures. A general characteristic of all filled systems measured was broadening of the tan δ peak due to the introduction of particulate matter into the polymeric matrix, which increased the number of modes of energy dissipation. Interfacial friction, particle–particle interactions, and altered polymer relaxation spectra have been shown to contribute to the increase of relative damping, especially near the transition region.[38]

Observed shifts of the 1 Hz tan δ peak temperatures are reported in Table IV. In general, these temperatures were raised by increasing the filler content.

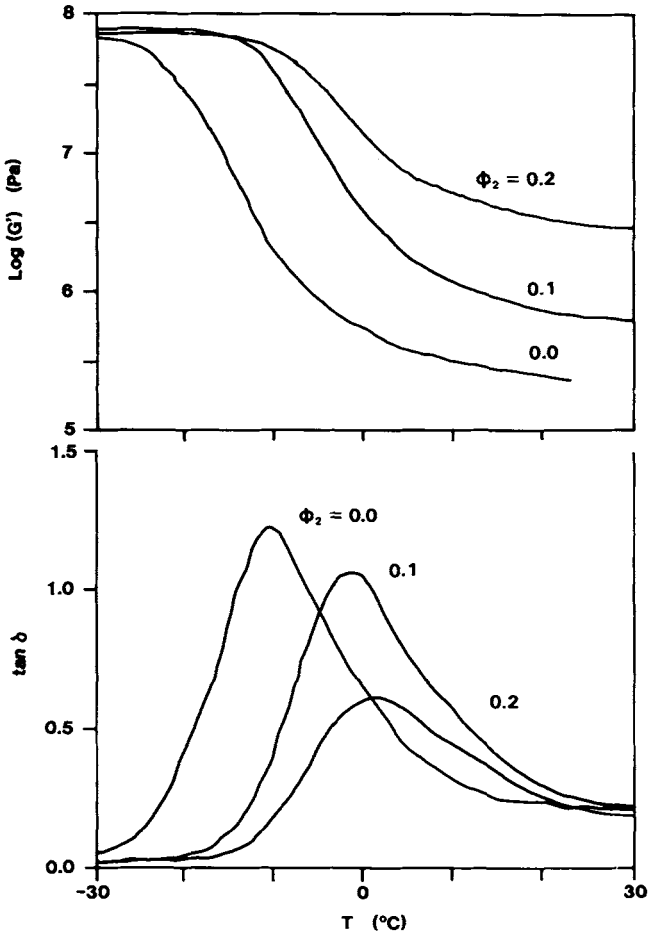

Fig. 2. Representative DMTA shear storage moduli (G') and tan δ data for the PEA–Extrusil system. Experimental conditions are as described in the text.

The G'' peak temperature shifts tended to parallel the tan δ peak shifts, although the former were generally greater. The maximum 1 Hz positive shifts of tan δ and G'' peak temperatures were 18 and 23°C, respectively, observed for the PAA–Durosil system. Large decreases of tan δ and G'' peak temperatures were observed for the PMA–OX50 system (−11 and −14°C, respectively at 1 Hz) and also to a lesser degree with PAA–OX50 and PMA–Durosil. Frequency was not a major factor in determining the magnitude of the T_g shift measured via DMTA. Data at the other frequencies closely resembled the general trends of the 1 Hz data. Linear correlations of ΔT_g with the logarithm of frequency for tan δ and G'' peaks were computed for every composite. The slopes of these correlations yielded a small positive slope, which for the tan δ data produced an increase of ΔT_g from 0 to 2°C per decade of frequency.

The DSC T_g values of both PEA and PMA unfilled homopolymer are also compared with previously reported data in Table III. The deviations of measured T_g from literature data for both polymers were equal for each of the

TABLE IV
Measured T_g Shifts

System	ϕ_2[a] =	ΔT_g (°C) 0.05	0.10	0.15	0.20
1 Hz tan δ peak					
OX50-PAA		−5 ± 1	−4 ± 1	−1 ± 2	0 ± 1
O-PMA		−8 ± 1	−11 ± 1	−10 ± 1	−9 ± 2
O-PEA		1 ± 1	0 ± 1	4 ± 1	1 ± 1
DUROSIL-PAA		3 ± 1	11 ± 1	13 ± 2	18 ± 1
D-PMA		−6 ± 2	−2 ± 1	2 ± 2	3 ± 1
D-PEA		0 ± 1	2 ± 1	2 ± 1	1 ± 2
EXTRUSIL-PAA		9 ± 1	14 ± 2	13 ± 1	15 ± 1
E-PMA		−1 ± 1	0 ± 1	5 ± 1	6 ± 2
E-PEA		8 ± 2	9 ± 1	10 ± 1	11 ± 1
DSC midpoint					
OX50-PMA		−0.5 ± 0.5	−0.5 ± 0.5	−0.1 ± 0.4	0.0 ± 0.6
O-PEA		−0.1 ± 0.7	0.3 ± 0.5		0.0 ± 0.8
DUROSIL-PMA		0.0 ± 0.5	−0.2 ± 0.6	0.0 ± 0.3	0.9 ± 0.4
D-PEA		0.8 ± 0.6	1.1 ± 0.5	1.8 ± 0.5	1.5 ± 0.6
EXTRUSIL-PMA		0.0 ± 0.7	1.0 ± 0.6	1.3 ± 0.8	1.2 ± 0.4
E-PEA		1.1 ± 0.7	1.2 ± 0.8	0.7 ± 0.9	1.0 ± 0.9

[a] Nominal volume fractions.

conventions used. This discrepancy is due to the tendency of DSC to shift observed transitions to higher temperatures at nonzero heating rates.[31,39,40] The errors associated with the DSC T_g values reported in Table III are the standard errors, computed from at least six measurements, plus a systematic calibration error of 0.5°C. Based upon scans to 200°C, no evidence of crystalline behavior was observed in the PEA and PMA samples.

Thermal histories are known to alter the measured T_g of polymers.[39] Peyser and Bascom[40] considered the effect of fillers upon T_g–cooling rate relationships and reported that the DSC determined ΔT_g increases with more rapid cooling rates for a polystyrene–silica system at constant filler content. Consequently, the thermal history behavior of the polymer composites was carefully evaluated to accurately determine changes in T_g. For unfilled PEA, DSC results showed the expected shift of midpoint T_g to lower temperatures with slower cooling rates, while the onset T_g was relatively insensitive to cooling rates. However, both the onset and midpoint ΔT_g of Extrusil filled PEA were found to increase with decreasing cooling rate, such that an additional T_g increase of approximately 1°C was obtained by decreasing the cooling rate from 100 to 2°C/min. This same trend has been observed earlier for an aluminum oxide filled PAA.[36] Based upon these results, and to facilitate comparison with the DMTA data, a DSC cooling rate of 10°C/min was maintained for all samples.

Midpoint T_g values of filled PEA and PMA are included in Table IV. The shift profiles measures by both onset and midpoint conventions were nearly identical. A maximum increase of DSC T_g of approximately 2°C was observed for PEA–Durosil while the maximum negative shift of T_g (−0.5°C) was observed for PMA–OX50. DMTA and DSC measured ΔT_g's for the

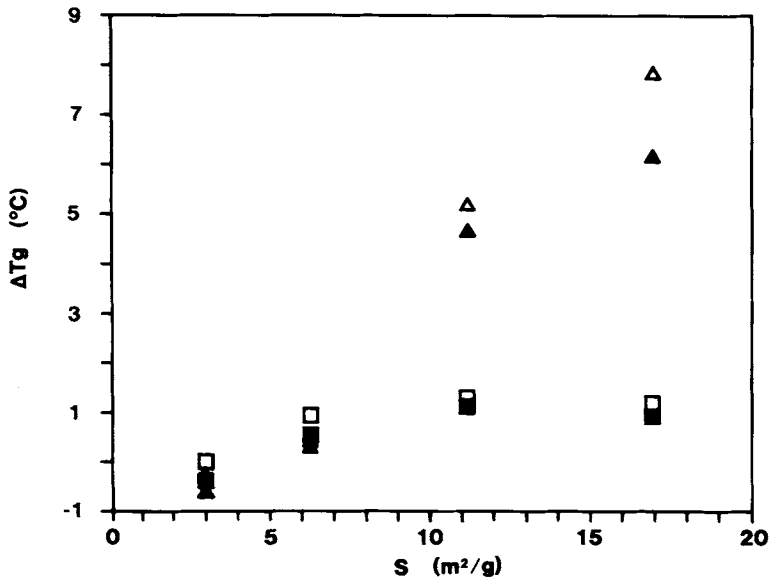

Fig. 3. Comparison of T_g shift for PMA–Extrusil obtained by DMTA tan δ peak (▲), G'' peak (△), DSC onset (■), and midpoint (□). S is the nominal particulate surface area per mass of polymer, which is introduced in eqs. (3) and (4) as a function of volume fraction.

PMA–Durosil systems are compared in Figure 3. T_g increases measured via DSC generally mirrored the trends obtained via DMTA but the magnitudes were lower by almost a factor of 10 for every PMA and PEA filter combination.

Due to changes of bulk thermal conductivity in filled polymer samples, small decreases of DSC T_g are possible. The thermal conductivity of amorphous silica is generally greater than amorphous polymer by an order of magnitude. This results in more rapid diffusion of heat throughout a filled sample, relative to unfilled, which produces lower transition temperatures with scanning thermal instruments. The magnitude of this effect is expected to be less than 1°C, deduced by observing the effect of DSC heating rate upon the measured T_g. Thus, the slight decreases of DSC T_g reported in Table IV may be related to the experimental technique. This effect was expected to be insignificant for DMTA measurements due to the slower heating rate.

Shear storage moduli at 1 Hz for the unfilled polymers (G_0') are reported in Table II. Measurements were made at temperatures with the same relative values (i.e., tan δ maximum plus 30°C), such that the composites were in the rubbery plateau region of mechanical behavior. Relative shear storage moduli ($G_r' = G'(\phi_2)/G_0'$), also measured at 30°C above the tan δ peak of the filled composites, are reported in Table V. The degree of reinforcement (modulus enhancement) depended on not only the volumetric content of filler, but also the type of interactions between the components, as $G_r'(\phi_2)$ differs for each system. Additionally, modulus enhancement was even observed for those systems where ΔT_g was negative.

TABLE V
Relative Modulus Values

System	ϕ_2[b] =	G_r'[a] 0.05	0.10	0.15	0.20
OX50-PAA		0.71	1.00	1.50	1.47
O-PMA		1.52	1.43	2.05	3.39
O-PEA		1.22	2.22	2.74	3.13
DUROSIL-PAA		0.76	1.20	2.29	3.02
D-PMA		1.51	2.34	5.37	7.59
D-PEA		0.93	1.32	2.45	4.37
EXTRUSIL-PAA		0.57	1.27	1.71	2.40
E-PMA		1.00	1.87	3.94	8.43
E-PEA		1.75	2.42	6.04	11.3

[a] $G_r' = G'(\phi_2)/G_0'$, at $\tan\delta(\phi_2)_{max}$ + 30°C, 1 Hz.
[b] Nominal volume fraction.

DISCUSSION

Even with carefully controlled experimental conditions, changes of T_g behavior for these silica filled acrylic systems (Table IV) tend to resemble the situation described by Figure 1. Nonetheless, the general trend of increased T_g with increasing amounts of filler is consistent with the concept of an interfacial region in which the polymer is bound to the filler surface. The measured magnitudes of T_g shifts additionally depended upon the measurement method as shown in Figure 3; ΔT_g was consistently greater when measured by DMTA, than by DSC. This suggests that there are modes of interaction between filler and matrix that are activated by mechanical and thermal means, independently.

Interaction of the interfacial region with the matrix material has been reported to extend from tens to thousands of angstroms from the particle surface.[2,3,5] This is partly due to additional chain entanglements from the presence of filler particles (hydrodynamic effects) and adsorbed polymeric segments which form temporary "crosslinks." As suggested by Chahal and St. Pierre,[41] "multi-segmental adsorption of entangled molecules," as well as adsorption of molecules which extend from one particle to another, are possible in composite systems.

Dynamic mechanical measurements detect polymer–filler surface interactions as well as long range entanglements of the affected molecules. The latter are manifested by the frequency contribution to ΔT_g, i.e., as frequency was increased, ΔT_g tended to increase slightly. On the other hand, DSC predominantly measures the segmental–surface interactions. Thus, we expect that $\Delta T_{g_{mech}} > \Delta T_{g_{therm}}$ due to the additional interaction mechanism involved in mechanical deformation. For either measurement method, the strength of these segmental–surface interactions depends upon sample thermal history. For example, when the DSC cooling rate was decreased by 2 decades for the filled PEA systems, the magnitude of ΔT_g was nearly doubled. Depending upon the specific time/temperature conditions below T_g, more interaction sites may form and existing sites may become more tightly bound, thereby contributing to an increased ΔT_g.

The decreases of the tan δ and G'' peak temperatures for the PMA–OX50 and –Durosil composites were not duplicated by DSC T_g measurements (Table IV). Indeed, the DSC results indicated no significant decrease of T_g greater than the instrument reproducibility. However, for PEA– and PMA–Extrusil composites, significant increases of T_g were detected via DSC which paralleled those measured by DMTA. T_g decreases which were detected via DMTA, but not DSC, are attributable to interparticle mechanical interactions. Therefore, an appropriate model of the complete ΔT_g behavior for the particulate-filled composites must take into account both matrix–filler as well as filler–filler interactions.

A relationship to describe the T_g behavior of filled polymers can be obtained by utilizing the adsorptional boundary layer concepts described above. Consider the T_g–crosslink density equation of Fox and Loshaek,[42]

$$T_g(c) = K_x C_2 \tag{2}$$

where $T_g(c)$ is the increase of T_g for a crosslinked polymer corrected for the copolymer effect, with C_2 crosslinks per mass of polymer, and K_x is a constant which depends upon the individual monomers. Mobility restrictions are introduced into the polymer chains by segmental adsorption onto filler surface sites, which we assume to be uniformly distributed over the available particulate surface. If these polymer–adsorption sites behave similarly to crosslink junctions, then the following equation can be formulated by analogy with eq. (2):

$$T_g(f) = K_0 S \tag{3}$$

In eq. (3), $T_g(f)$ is the glass transition temperature increase of the filled polymer [identical to ΔT_g defined in eq. (1)], S is the surface area of filler per unit mass of polymer, and K_0 is a material constant depending upon the specific nature of the components. This equation is similar in form to one proposed by Iisaka and Shibayam.[12] By expressing S in terms of a constant specific surface area $\bar{s}$ (i.e., surface area per unit mass of filler), the following is obtained:

$$\Delta T_g = K_0 \bar{s} m_2/m_1$$

or

$$\Delta T_g = K_0 \bar{s}(d_2/d_1)[\phi_2/(1 - \phi_2)] \tag{4}$$

where m_i and d_i are the mass fractions and densities, respectively, of polymer ($i = 1$) and filler ($i = 2$).

Equation (4) now gives justification for a functional dependence of T_g upon ϕ_2 with specific polymer–filler interactions embedded in the constant K_0. Utilizing this relationship, a linear regression analysis was conducted for the entire set of DMTA and DSC T_g shift data, the results of which are reported in Table IV. As the unfilled polymer reference point ($\Delta T_g = 0$) represents an entirely different physical system relative to the respective filled materials, it was not included in this analysis; however, data were incorporated from the full DMTA frequency spectrum.

TABLE VI
Statistical Analysis of $T_g(\phi_2)$ Dependence According to Eq. (4):
$\Delta T_g = A_0 + K_0\bar{s}(d_2/d_1)[\phi_2/(1 - \phi_2)]$

System	n[a]	A_0 (°C)	$K_0 \pm$ err. ($\times 10^3$) (g °C/m^2)	p[b]	A_0 (°C)	$K_0 \pm$ err. ($\times 10^3$) (g °C/m^2)	p
		Tan δ peaks			G'' peaks		
O-PAA	46	−5	350 ± 50	< 0.001	−3	350 ± 30	< 0.001
O-PMA	87	−8	−66 ± 30	0.03	−8	−320 ± 40	< 0.001
O-PEA	46	1	52 ± 50	ns[c]	1	100 ± 60	0.08
D-PAA	48	2	820 ± 70	< 0.001	1	1100 ± 60	< 0.001
D-PMA	80	−8	520 ± 20	< 0.001	−7	550 ± 20	< 0.001
D-PEA	48	0	86 ± 26	< 0.001	−2	230 ± 30	< 0.001
E-PAA	45	10	520 ± 90	< 0.001	8	850 ± 70	< 0.001
E-PMA	80	−3	610 ± 30	< 0.001	−2	610 ± 20	< 0.001
E-PEA	68	7	350 ± 50	< 0.001	9	340 ± 50	< 0.001
		DSC midpoint T_g			DSC onset T_g		
O-PMA	14	−0.7	32 ± 18	0.09	−0.9	24 ± 23	ns
O-PEA	9	0.2	−4 ± 23	ns	0.4	5 ± 18	ns
D-PMA	13	−0.4	48 ± 18	0.02	−0.4	36 ± 17	0.05
D-PEA	17	0.8	31 ± 12	0.03	1.1	19 ± 15	ns
E-PMA	13	0.1	82 ± 40	0.06	−0.4	99 ± 44	0.05
E-PEA	12	1.2	−21 ± 50	ns	0.7	32 ± 32	ns

[a] Number of measurements.
[b] Analysis of variance probability of error unexplained by regression.
[c] Not significant, $p > 0.1$.

The effect of the polymer pendant group polarity upon the magnitude of the T_g shift can be described in terms of systematic changes in K_0 [eq. (4)]. Interaction of acrylic polymers with metallic oxide surfaces has been shown via infrared and Mössbauer spectroscopy by Leidheiser and Deck[43] to occur via the carbonyl group. For the case of silica, interaction occurs via hydrogen bonding between the silanol and the carbonyl groups. For the acrylics investigated in our study, PAA is the most polar and has the greatest carbonyl mobility for interaction with silica. As the length of the ester is increased, the mobility of the carbonyl decreases due to steric hindrance and the amount of silica interaction is correspondingly decreased. For example, with the Durosil filled composites, the values of tan δ K_0 decreased monotonically from 0.8 for PAA (most polar) to 0.09 for PEA (least polar), and similar values were observed for G'' (Table VI). The Extrusil and OX50 composites also evidenced a decrease of K_0 with decreasing pendant polarity for both tan δ and G'', with the exception of the PMA–OX50 system. The DSC values of K_0 similarly decreased between PMA and PEA for all three fillers and both measurement techniques.

These results indicated that the T_g shift of a particulate composite is greater as the interaction between the matrix and filler becomes stronger. Fowkes[44] has shown that polymer adsorption onto filler surface will be greater when there is a difference between their respective acid–base parameters. The surface nature for all of the fillers investigated is "acidic" due to the presence of the silanol groups. PMA is a relatively "basic" polymer due to the nature of

the carbonyl group,[44] but PEA is less "basic" due to the additional length of the ester. Thus, greater interaction is expected between PMA and silica than with PEA and silica due to the acid–base differences. In addition, interaction of PMA and PEA with the precipitated silica (Durosil and Extrusil) should be greater than fumed silica due the higher silanol concentration. These characteristics are generally reflected in the values of K_0 (Table VI).

The interaction of PAA with these silicas is more complicated than described above due to the formation of carboxylate ions during processing of the PAA composites in ethanol. Matsuura and Eisenberg[45] have demonstrated that the addition of Na or Ca ions to poly(EA-co-AA) increases the T_g due to ionomer formation. Since Durosil and Extrusil contain Na and Ca on the surface, ionic interactions are possible. Additionally, these ions may be transported beyond the surface into the surrounding matrix over time.[43] Based upon this mechanism, the boundary layer formed about particles may be more tightly bound and may therefore possess a higher T_g than similar composites fabricated in absence of these ions, such as the PAA–OX50 materials. This may explain why the ΔT_g's for the PAA composites were much greater for the precipitated silicas than for the fumed silica (Table IV).

There are certain aspects of filled polymer T_g behavior that are not addressed by this adsorptional-crosslinking approach. For example, the nonzero values of the intercepts (A_0) computed from the linear regressions (Table VI) indicate that the first increments of filler introduced into polymer matrix have a much greater effect than subsequent amounts, especially for those samples in which T_g initially decreased. For certain systems such as the PAA–Extrusil composites, ΔT_g increases substantially, and then decreased, with increasing filler content. Other investigators have noted that T_g tends to asymptotically approach a constant value at very high loadings.[3,4,46] Thus, a simple relationship such as eq. (4) does not adequately account for the observed nonlinear nature of T_g behavior, especially for lower ($\phi_2 < 0.05$) or higher ($\phi_2 > 0.2$) filler loadings.

Examination of the microstructure of these acrylic composites via transmission electron microscopy has indicated that a significant degree of agglomeration occurs with the submicron fillers. Figure 4 is a TEM micrograph of one of the PAA–Durosil composites studied. Although Durosil is designed for good dispersion in rubber matrices by the shearing of aggregates on a roll mill, the sonic processing used in this study did not completely disrupt these aggregates. In Figure 4, individual particles can be discerned, but aggregates as large as 5 μm in diameter were also observed in the same sample. Therefore, there is reason to believe that the specific surface area term ($\bar{s}$) in eq. (4) is not a constant for a given series of polymer and fillers, but varies with filler content.

Equation (4) can be modified to reflect the amount of particulate surface area actually available for polymer absorption by multiplying $\bar{s}$ with the term $A_p(\phi_2)$, which represents the area fraction of filler surface that is in contact with polymer (as opposed to internal or interparticle surface). This term can be determined directly by measurements of polymer–filler composites. The exact functional form of $A_p(\phi_2)$ has not yet been evaluated, but is expected to be nonlinear, approaching a nonzero constant as $\phi_2 \rightarrow 0$ (dependent upon the

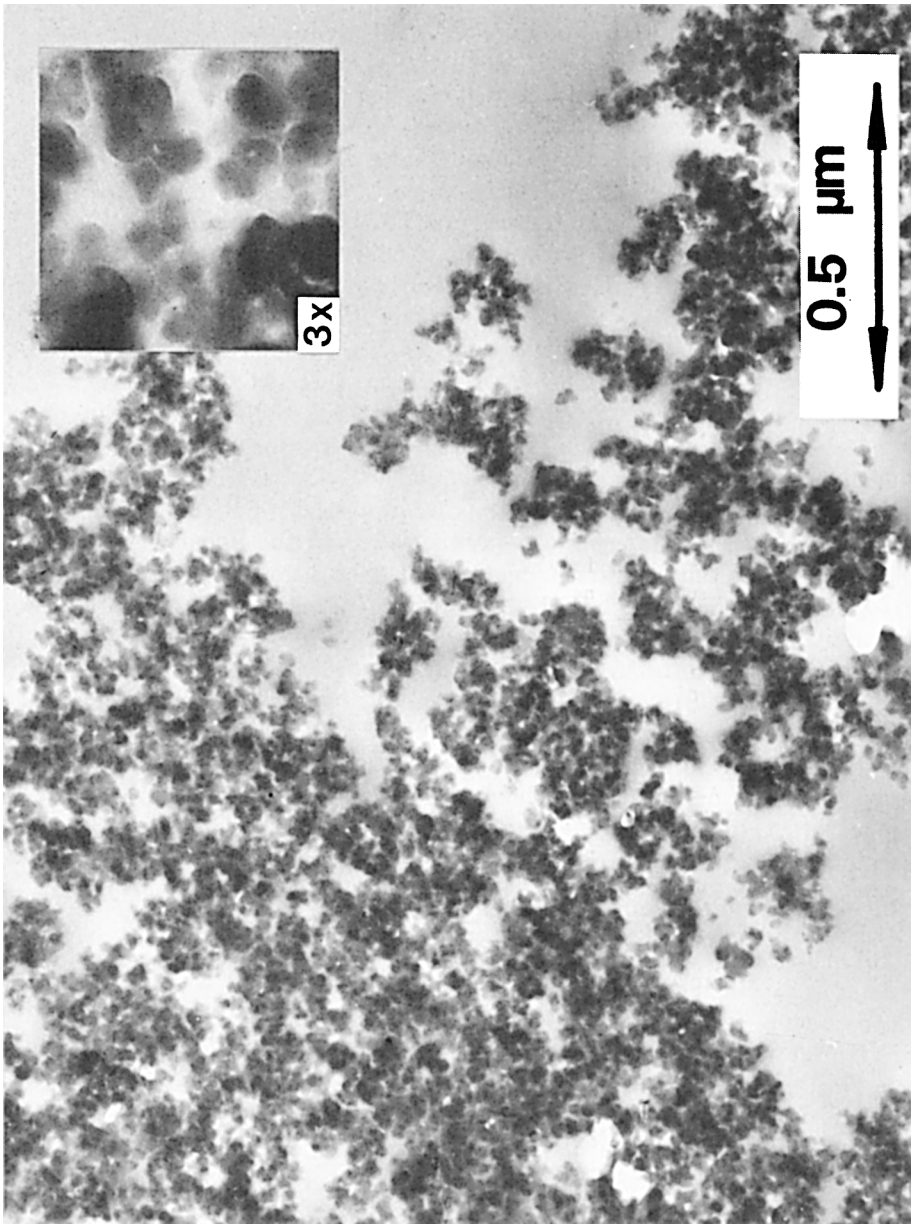

Fig. 4. Representative TEM micrograph of a 0.1 μm thick section of a PAA–Durosil composite ($\phi_2 = 0.11$). Sample fabrication was as described in the text. The specimen was microtomed after encapsulation in a nonpenetrating epoxy. The 0.5 μm arrow also represents approximately 20 primary particle diameters. The micrograph clearly indicates that extensive particulate agglomeration still exists despite sonic agitation during processing.

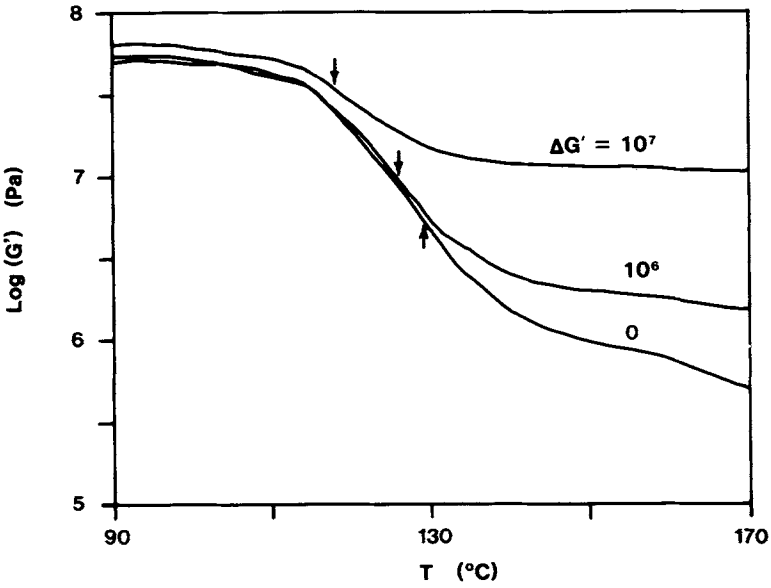

Fig. 5. Schematic representing model behavior of the shear storage modulus (G') for an unfilled PAA. The term $\Delta G'$, which represents a modulus enhancement term due to filler–filler linkages at an arbitrary low strain value, has been added arithmetically to the nominal G' transition curve. The inflection point (↓), which is associated with T_g, is shifted to lower temperatures with increasing $\Delta G'$. Thus, filler–filler linkages may possibly contribute to a depression of T_g when measured by dynamic mechanical means.

structure of the filler), and approaching zero as ϕ_2 approaches the random sphere packing factor of 0.6. Hence, by incorporating $A_p(\phi_2)$ into eq. (4), the nonlinear positive ΔT_g behavior, such as subsequent decreases and asymptotic approaches of T_g, can be accommodated. Although this modification represents a major improvement in the model, it does not describe the observed negative values of ΔT_g.

This shortcoming arises because the above analysis has not considered possible filler–filler interactions within the composite. The mechanical T_g is related to energy dissipation and storage characteristics of the composite, which are influenced by particle–particle motion.[38] These motions should therefore contribute to mechanical T_g shifts. Payne has described the strain amplitude dependence of the storage modulus for particulate filled elastomers as due to elastic filler–filler linkages (e.g., Ref. 47 and review by Medalia[48]). Kraus[49] has developed a model of this behavior by considering a van der Walls network of filler particles. The contribution to the dynamic moduli of filled elastomers from this mechanism is additive arithmetically, not logarithmically, as evident from observations.[47]

A consequence of this filler–filler mechanism is that viscoelastic spectra which closely resemble temperature dependent spectra are observed as a function of the logarithm of strain.[49] Because the log-strain spectra change with temperature, the temperature spectra of filled polymers will consequently change with strain level. Possible consequences of this phenomenon are presented in Figure 5. This schematic represents the arithmetic addition of a particle–particle modulus term ($\Delta G'$) for a hypothetical small strain defor-

mation to the temperature-dependent storage modulus of unfilled PAA (Fig. 5). As $\Delta G'$ becomes larger (greater particle–particle interaction), the inflection point of the $\log[G'(\phi_2, T)]$ curves, another convention for mechanical T_g, is displaced to lower temperatures. Thus, filler–filler interactions or the "Payne effect"[48] may contribute to the decrease of T_g when measured by small strain dynamic mechanical methods.

Based upon the preceding discussion, eq. (4) must be modified to allow for depression of T_g by filler–filler interactions. If the total change of mechanical T_g is now assumed to be due to the additive effects of the polymer–filler and filler–filler ($\Delta T_{g_{ff}}$) shifts, then eq. (4) is transformed to

$$\Delta T_g = K_0 A_p(\phi_2)\bar{s}(d_2/d_1)[\phi_2/(1 - \phi_2)] - \Delta T_{g_{ff}} \tag{5}$$

where the $A_p(\phi_2)$ term has also been included. Experimental verification of mechanical T_g depression by filler–filler interactions can be determined by varying the dynamic strain amplitude. Preliminary modeling calculations suggest a logarithmic dependence of $\Delta T_{g_{ff}}$ upon the level of modulus enhancement due to filler–filler contributions. By the addition of such a nonlinear term, eq. (5) should allow the complete range of observed ΔT_g behavior to be explained.

SUMMARY

The glass transition temperatures for silica- and silicate-filled PAA, PMA, and PEA were observed to shift in directions and by magnitudes which depended upon the nature of the specific composite components as well as the measurement technique. Although both increases and decreases in T_g were observed via dynamic mechanical measurements, no statistically significant decreases were obtained with DSC. A maximum positive shift of the 1 Hz $\tan\delta$ peak of 18°C was observed for the PAA–Durosil system ($\phi_2 = 0.2$), while a maximum negative shift of −11°C was observed in the PMA–OX50 system ($\phi_2 = 0.1$). Relative modulus values indicated that a mechanical reinforcing effects occurred in all systems, even those in which T_g decreases were observed.

Based upon these results, a model was proposed which incorporated a positive contribution to T_g shifts from matrix–filler interactions, and a negative contribution from filler–filler interactions. By considering the matrix–filler contribution only, evaluation of the data in terms of a $\Delta T_g(\phi_2)$ functional dependence suggested that matrix–filler interactions were enhanced when the relative electrostatic differences between polymer and filler were increased.

This research was conducted with financial support provided by the Gates Rubber Company of Denver, Colorado. We gratefully acknowledge the assistance of Douglas Schneider of Gates Research and Development for providing GPC measurements, and M. Douglas Wray of the University of Colarado for his assistance with electron microscopy.

References

1. J. B. Donnet and A. Vidal, in *Advances in Polymer Science*, K. Dusek, Ed., Springer-Verlag, Berlin, 1986, Vol. 76, pp. 103–127.
2. Y. S. Lipatov, *Physical Chemistry of Filled Polymers*, International Polymer Science and Technology Monograph No. 2, R. J. Moseley, transl., Rubber and Plastics Research Association of Great Britain, Shawbury, U.K., 1979.
3. D. H. Droste and A. T. DiBenedetto, *J. Appl. Polym. Sci.*, **13,** 2149 (1969).
4. G. Fritschy and E. Papirer, *J. Appl. Polym. Sci.*, **25,** 1867 (1980).
5. A. Yim, R. S. Chahal, and L. E. St. Pierre, *J. Colloid Interface Sci.*, **43,** 583 (1973).
6. A. Eisenberg, in *Physical Properties of Polymers*, J. E. Mark, Ed., American Chemical Society, Washington, DC, 1984, pp. 55–95.
7. L. E. Nielsen, *J. Macromol. Sci., Rev. Macromol. Chem.*, **C3,** 69 (1969).
8. S. Kaufman, W. P. Slichter, and D. D. Davis, *J. Polym. Sci. A*-2, **9,** 829 (1971).
9. E. Price, D. M. French, and A. S. Tompa, *J. Appl. Polym. Sci.*, **16,** 157 (1972).
10. J. A. Manson and L. H. Sperling, *Polymer Blends and Composites*, Plenum, New York, 1976.
11. G. J. Howard and R. A. Shanks, *J. Appl. Polym. Sci.*, **26,** 3099 (1981).
12. K. Iisaka and K. Shibayama, *J. Appl. Polym. Sci.*, **22,** 1321 (1978).
13. R. F. Landel and T. L. Smith, *Am. Rocket Soc. J.*, **31,** 599 (1961).
14. Y. S. Lipatov, in *Advances in Polymer Science*, H. J. Cantow, Ed., Springer-Verlag, Berlin, 1977, Vol. 22, pp. 1–59.
15. A. Yim and L. E. St. Pierre, *Polym. Lett.*, **7,** 237 (1969).
16. A. R. Greenberg, *J. Mater. Sci. Lett.*, **6,** 78 (1987).
17. G. Kraus and J. T. Gruver, *J. Polym. Sci. A*-2, **8,** 571 (1970).
18. J. Kolarik and J. Janacek, *J. Appl. Polym. Sci.*, **20,** 841 (1976).
19. C. W. van der Waal, H. W. Bree, and F. R. Schwarzl, *J. Appl. Polym. Sci.*, **9,** 2143 (1965).
20. A. Toussaint, *Prog. Org. Coat.*, **2,** 237 (1973/74).
21. G. J. Howard and R. A. Shanks, *J. Macromol. Sci. Chem.*, **A17,** 287 (1982).
22. P. V. T. Raghuram and U. S. Nandi, *J. Polym. Sci. A*-1, **8,** 3079 (1970).
23. *Product Brochure*: *Precipitated Silicas and Silicates, Manufacture, Properties and Applications* (1984), Degussa Corporation, Pigments Division, Ridgefield Park, NJ.
24. *Technical Bulletin Pigments No.* 16: *Analytical Methods for Synthetic Silicas and Silicates* (1978), Degussa Corporation, Pigments Division, Ridgefield Park, NJ.
25. *Technical Bulletin Pigments No* 32: *Amorphous Synthetic Silica Products in Powder Form, Production and Characterization* (1980), Degussa Corporation, Pigments Division, Teterboro, NJ.
26. S. K. Wason, in *Handbook of Fillers for Plastics*, H. S. Katz and J. V. Milewski, Eds., New York, Van Nostrand Reinhold, 1987, pp. 165–201.
27. E. M. Dannenberg, *Rubber Chem. Technol.*, **55,** 860 (1982).
28. A. Voet, *J. Polym. Sci., Macromol. Rev.*, **15,** 327 (1980).
29. R. K. Iler, *The Chemistry of Silica*, New York, Wiley-Interscience, 1979, pp. 462–621.
30. A. R. Greenberg and I. Kamel, *J. Polym. Sci. Polym. Chem. Ed.*, **15,** 2137 (1977).
31. J. H. Flynn, *Thermochim. Acta*, **8,** 69 (1974).
32. J. Heijboer, in *Physics of Non-Crystalline Solids*, J. A. Prins, Ed., North-Holland, Amsterdam, 1965, pp. 231–254.
33. V. H. Thurn and K. Wolf, *Kolloid Z.*, **148,** 16 (1956).
34. A. R. Greenberg and M. Messaros, *Polym. Prepr.*, **26** (1), 28 (1985).
35. J. Kolarik, *J. Appl. Polym. Sci.*, **24,** 1565 (1979).
36. C. G. Reid and A. R. Greenberg, *Proc. 14th N. Am. Therm. Anal. Soc. Conf.*, B. B. Chowdhury, Ed., 1985, Vol. 14, p. 67.
37. W. A. Lee and R. A. Rutherford, in *Polymer Handbook*, 2nd ed., J. Brandrup and E. H. Immergut, Eds., Wiley, New York, 1975, p. (III) 139.
38. L. E. Nielsen, *Mechanical Properties of Polymers and Composites*, Dekker, New York, 1974, Vol. 2, pp. 379–452.

39. B. Wunderlich, D. M. Bodily, and M. H. Kaplan, *J. Appl. Phys.*, **35,** 95 (1964).
40. P. Peyser and W. D. Bascom, *J. Macromol. Sci. Phys.*, **B13,** 597 (1977).
41. R. S. Chahal and L. E. St. Pierre, *Macromolecules*, **2,** 193 (1969).
42. T. G. Fox and S. Loshaek, *J. Polym. Sci.*, **15,** 371 (1955).
43. H. Leidheiser, Jr., and P. D. Deck, *Science*, **241,** 1176 (1988).
44. F. M. Fowkes, *Rubber Chem. Technol.*, **57,** 328 (1984).
45. H. Matsuura and A. Eisenberg, *J. Polym. Sci. Polym. Phys. Ed.*, **14,** 1201 (1976).
46. L. Aras, R. P. Sheldon, and H. M. Lai, *J. Polym. Sci. Polym. Lett. Ed.*, **16,** 27 (1978).
47. A. R. Payne, in *Reinforcement of Elastomers*, G. Kraus, Ed., Wiley-Interscience, New York, 1965, pp. 69–123.
48. A. I. Medalia, in Elastomers: *Criteria for Engineering Design*, C. Hepburn and R. J. W. Reynolds, Eds., Applied Science, London, 1979, pp. 257–272.
49. G. Kraus, *J. Appl. Polym. Sci.*, **39,** 75 (1984).

Received February 15, 1989
Accepted February 21, 1989